Stochastic approach to plasticity and yield in amorphous solids

H. G. E. Hentschel,[1,2] Prabhat K. Jaiswal,[1] Itamar Procaccia,[1] and Srikanth Sastry[3]
[1]*Department of Chemical Physics, Weizmann Institute of Science, Rehovot 76100, Israel*
[2]*Department of Physics, Emory University, Atlanta, Georgia, United States*
[3]*Jawaharlal Nehru Centre for Advanced Scientific Research, Jakkur Campus, Bangalore 560064, India*
(Received 16 September 2015; published 4 December 2015)

We focus on the probability distribution function (PDF) $P(\Delta\gamma;\gamma)$ where $\Delta\gamma$ are the *measured* strain intervals between plastic events in a athermal strained amorphous solids, and γ measures the accumulated strain. The tail of this distribution as $\Delta\gamma \to 0$ (in the thermodynamic limit) scales like $\Delta\gamma^{\eta}$. The exponent η is related via scaling relations to the tail of the PDF of the eigenvalues of the *plastic modes* of the Hessian matrix $P(\lambda)$ which scales like λ^{θ}, $\eta = (\theta - 1)/2$. The numerical values of η or θ can be determined easily in the unstrained material and in the yielded state of plastic flow. Special care is called for in the determination of these exponents between these states as γ increases. Determining the γ dependence of the PDF $P(\Delta\gamma;\gamma)$ can shed important light on plasticity and yield. We conclude that the PDF's of both $\Delta\gamma$ and λ are not continuous functions of γ. In slowly quenched amorphous solids they undergo two discontinuous transitions, first at $\gamma = 0^{+}$ and then at the yield point $\gamma = \gamma_{Y}$ to plastic flow. In quickly quenched amorphous solids the second transition is smeared out due to the nonexisting stress peak before yield. The nature of these transitions and scaling relations with the system size dependence of $\langle\Delta\gamma\rangle$ are discussed.

DOI: 10.1103/PhysRevE.92.062302 PACS number(s): 46.35.+z, 61.43.Dq, 83.80.Ab

I. INTRODUCTION

Amorphous solids are materials lacking any crystalline order that exhibit a finite shear modulus when strained. When the material is shear driven, the relations between the stress and the strain (in quasistatic conditions) or between the stress and strain rate (in dynamical condition) has been studied extensively by many groups [1,2]. Such studies have been conducted in both thermal and athermal conditions, where the latter refer to situations where thermal fluctuations are irrelevant. One learns that the response to external strain in amorphous solids as the strain γ is increased in an athermal quasistatic (AQS) manner does not result in a smooth differentiable stress-strain relationship. Rather, it results in a sequence of reversible strain increases $\Delta\gamma_1, \Delta\gamma_2, \Delta\gamma_3, \ldots$ followed in each case by an irreversible plastic event in which a local, subextensive, or extensive group of particles dissipate energy and the system then falls into a new inherent state. After each such event $\Delta\gamma_i$ the stress has changed by $\Delta\sigma_i$. An ensemble of sufficiently many independent realizations of this process at any value of γ will then give rise to a probability distribution function (PDF) $P(\Delta\gamma;\gamma)$. The properties of this PDF and in particular of the scaling form of the tail of this PDF as $\Delta\gamma \to 0$ were the subject of focused recent research. The tail of the distribution is relevant for the thermodynamic limit since the intervals $\Delta\gamma_i$ shrink when the system size increases as shown below [Eq. (2)].

In Ref. [3] it was shown that for $\gamma = 0$, i.e., after a quench from the liquid state to the amorphous state at $T = 0$, the tail of the PDF appears to scale like

$$\lim_{\Delta\gamma\to 0} P(\Delta\gamma, \gamma = 0) \sim (\Delta\gamma)^{\eta} . \tag{1}$$

The exponent η was measured there to be $\eta \approx 0.6$ in two dimensions without any claim for universality; in particular this exponent may depend on the quench rate from the liquid to the solid. Besides the presence of a scaling tail it was shown that the whole PDF agrees extremely well with the Weibull distribution, giving rise to an interesting scaling relation to the *system size* dependence of the mean value of $\Delta\gamma$ at $\gamma = 0$,

$$\langle\Delta\gamma\rangle \sim N^{\beta}, \quad \beta < 0 . \tag{2}$$

The scaling relation follows from the theory of extreme value statistics, and with the Weibull form it reads [3]

$$\beta = -\frac{1}{1+\eta}, \quad \eta = -\left(1 + \frac{1}{\beta}\right). \tag{3}$$

Indeed, the exponent β was found to be in perfect consistency with $\eta \approx 0.6$, i.e., $\beta \approx -0.62$. The method of measurement employed many independent realizations of quenched systems at $\gamma = 0$. It is important to stress that for large systems the mean value $\langle\Delta\gamma\rangle$ tends to decrease with system size according to Eq. (2). The scaling presented in Eq. (1) refers always to values of $\Delta\gamma \ll \langle\Delta\gamma\rangle$.

Other statistically stable scaling relations can be obtained in the steady-state plastic flow after the plastic yield. Here we have many repeated events in stationary conditions, allowing us to measure carefully the statistics of energy drops ΔU_i, stress drops $\Delta\sigma_i$, and strain intervals $\delta\gamma_i$. It was found numerically in Ref. [4] and then analytically in Ref. [3] that

$$\langle\Delta U\rangle = \bar{\epsilon} N^{\alpha}, \quad \langle\Delta\sigma\rangle = \bar{s} N^{\beta}, \quad \langle\Delta\gamma\rangle = N^{\beta}, \tag{4}$$

with $\alpha = 1/3$ and $\beta = -2/3$ as exact universal results. On the other hand it was shown that the relation (3) is no longer valid in the plastic flow state; in fact, there $\eta = 0$ and the PDF has no relation to the Weibull distribution. This major difference was ascribed to the existence of subextensive plastic events in the plastic flow steady state. These subextensive events are correlated, destroying the statistical independence of repeated realizations in the quenched $\gamma = 0$ state which is necessary for the scaling laws (3).

The changes in the statistical properties as they are reflected in the PDF of the strain intervals $\Delta\gamma$ raise an interesting challenge. Can one follow these changes to understand plasticity

in amorphous solids, and in particular to study the yielding transition to the steady-state plastic flow. This challenge was picked up in particular in Refs. [5,6]. The upshot of these studies is that there exists a continuous change, as a function of the external strain γ, of the values of the scaling exponent, from $\gamma = 0$ to the plastic flow regime. If correct this would supply an extremely rare occasion of a continuous change in a scaling exponent as a function of a control parameter [7]. The aim of this paper is to study carefully this interesting proposition. We end up offering a different point of view in which we stress two discontinuous transitions, one at $\gamma = 0^+$ and the other at the yield point $\gamma = \gamma_Y$. It should be pointed out, however, that in this paper we discuss only the measurable strain intervals between plastic events and the lowest eigenvalues of the Hessian matrix that vanish during the approach to a plastic events. In Refs. [5,6] there appear distributions of variables that are not readily measurable in strained amorphous solids, and a full comparison of predictions is not always easy. Nevertheless our conclusion that the yield is a discontinuous transition (at least in slowly quenched amorphous solids) is in accordance with recent studies that have used very different methods of investigation [8].

In Sec. II we present some numerical estimates of the exponent β and of the PDF $P(\Delta\gamma;\gamma)$ for a range of values of the external strain γ. To interpret properly the numerical results we turn in Sec. III to theoretical consideration. These considerations are based on relating the scaling properties of $P(\Delta\gamma;\gamma)$ to the scaling properties of another PDF, $P(\lambda;\gamma)$, which describes the distribution of eigenvalues of the *plastic modes* of the Hessian matrix, precisely those eigenvalues that approach zero before a plastic event is taking place. The separation into Debye modes and plastic modes was justified in Refs. [9–11]; see also Ref. [12]. In Sec. III we present a Fokker-Planck equation for the development of $P(\lambda;\gamma)$ as a function of increasing γ. While we cannot vouch for the exactness of this equation, we argue that the scaling properties of this equation are robust and can be trusted to provide the correct scaling exponents for the tails of $P(\lambda;\gamma)$ and $P(\Delta\gamma;\gamma)$. In Sec. IV we offer a summary and conclusions.

II. DIRECT NUMERICAL RESULTS

In this section we describe direct numerical measurements of the exponent β and η. To generate data we have employed a 50-50 binary mixture of point particles interacting via the Lennard-Jones potential in two dimensions. The parameters of the model can be found in Ref. [13]. The system is quenched from a high-temperature liquid to a target temperature $T = 0.001$ in Lennard-Jones units. We use two quench rates. In the first set of simulations the quench is "infinitely fast" in the sense that we use conjugate gradient energy minimization. In the second we reduce the temperature at a rate of 10^{-5} in Lennard-Jones units (cf. Ref. [4]), and we refer to it below as the "slow" quench. The mechanical properties of the differently quenched systems differ. The slow quench shows a distinct stress peak when γ is increased, followed by a yield toward the steady-state plastic flow. The fast quench results in a gradual increase in stress towards the plastic flow steady state without a stress peak. At $T = 0.001$ the temperature fluctuations are so small that they do not influence the mechanical properties. We refer to straining at this temperature as "athermal."

After preparing the system in athermal condition we follow the standard AQS protocol to strain the system in simple shear strain. We carefully measured the strain intervals $\Delta\gamma_i$ that occurred between plastic events. We back-tracked our simulations to increase the precision of this measurements (cf. Appendix of Ref. [4]). Every such simulation was repeated using 1000–1500 freshly quenched independent realizations. We have measured the distribution of $\Delta\gamma_i$ and the mean value $\langle\Delta\gamma\rangle$ as a function of N for different system sizes. While there is no ambiguity about the latter quantity at $\gamma = 0$, for higher values of γ we need to collect data within a bin of values of γ. We opted to do so in bins of size 0.01. Thus where we report below a value of γ, say, $\gamma = 0.02$ one needs to interpret that as data collected from all events that occur between $\gamma = 0.01$ and $\gamma = 0.02$.

In Fig. 1 we show some representative results for the measurement of the exponent β. In the upper panel the scaling law (2) is demonstrated for $\gamma = 0$, whereas in the lower panels we show the result for $\gamma = 0.04$ and $\gamma = 0.1$. The first one is in agreement with the previous estimate of $\beta \approx -0.62$. The last one is beyond the plastic yield and is in agreement with the exact prediction $\beta = -2/3$. The middle panel is an example of the new numbers obtained here for the first time for intermediate values of γ. An overall impression of the resulting picture can be obtained *if we assume that the scaling law (3) is obeyed throughout the range of* γ. We can then use the measurement of β to plot $-(1+\frac{1}{\beta})$ as a function of γ; see Fig. 2. If one believes that this represents the exponent η according to (3), then this continuous variation a function of γ is somewhat reminiscent of the dependence of this exponent on γ as predicted in Refs. [5,6] (this exponent is denoted as θ there). In fact we will argue now the following: (i) The scaling law (3) is valid only as long as $\gamma < \gamma_Y$. (ii) The measured values of β for $0 < \gamma < \gamma_Y$ suffer from severe finite size and crossover effects. In fact, the analysis presented below indicates that $\eta = 0$ and $\beta = -1$ for all the values of γ in the range $0 < \gamma < \gamma_Y$, with a transition to $\beta = -2/3$ after the plastic yield transition. The transition is expected to be sharp in the case of the slow quench, but much more smeared out in the case of the fast quench.

To see that the scaling law (3) fails for $\gamma > \gamma_Y$ it is sufficient to examine the PDF's $P(\Delta\gamma;\gamma)$. In Fig. 3 we present these distribution functions for the slowly quenched amorphous solid for a range of γ values starting with $\gamma = 0$ and ending with $\gamma = 0.09$, which is already beyond the plastic yield which for the present slowly quenched system is estimated at $\gamma_Y \approx 0.06$. It is clear that for $\gamma = 0$ the PDF has a perfect Weibull form with $\eta \approx 0.6$ in agreement with $\beta \approx -0.62$. But for all $\gamma > 0$ the PDF has a flat tail as $\Delta\gamma \to 0$, indicating a value of $\eta = 0$. In the plastic flow state, at $\gamma > \gamma_Y$, where we measure $\beta = -2/3$, the scaling law (3) is not obeyed. It was proposed in Ref. [3] that this is due to the subextensive plastic events that occur in the flowing state. The arguments leading to the scaling law (3) fail under these conditions.

The question is then whether the scaling law (3) holds in the range $\gamma < \gamma_Y$. We will argue that the answer is in the affirmative. We read $\eta = 0$ from the results of Fig. 3, and we propose that the correct value of β is $\beta = -1$, in agreement

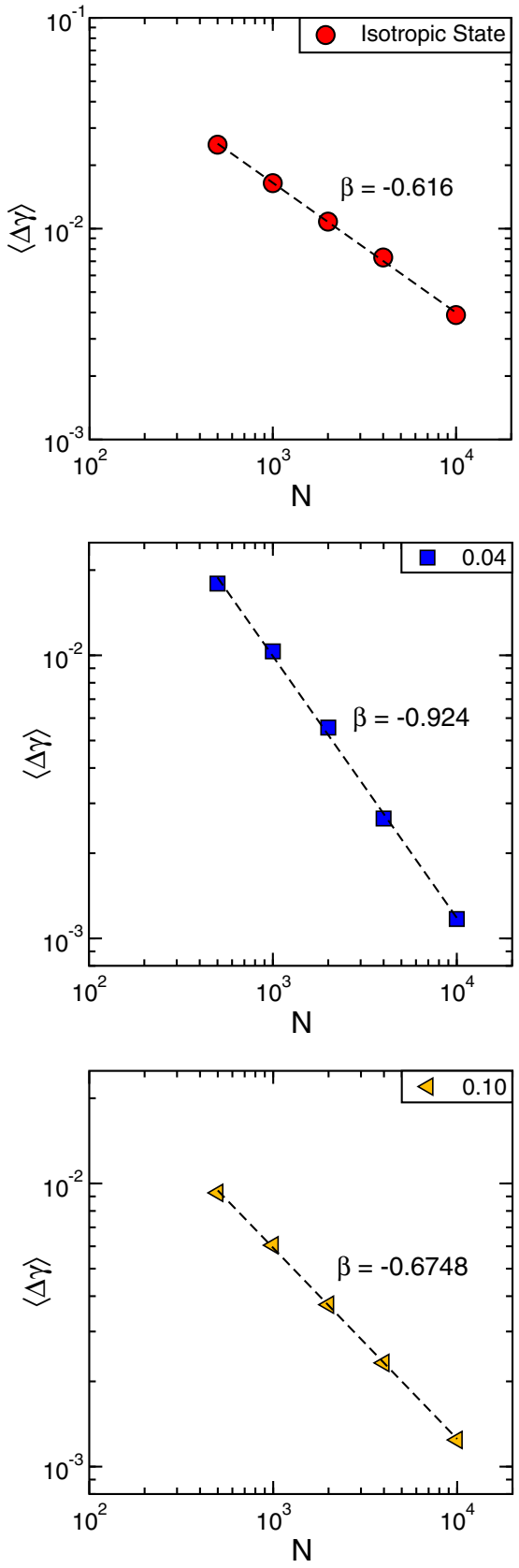

FIG. 1. (Color online) The scaling law (2) demonstrated for $\gamma = 0$ (upper panel), $\gamma = 0.04$ (middle panel), and $\gamma = 0.1$ (lower panel). We propose that in the range $0 < \gamma < \gamma_Y$ the value of β in the thermodynamic limit is $\beta = -1$.

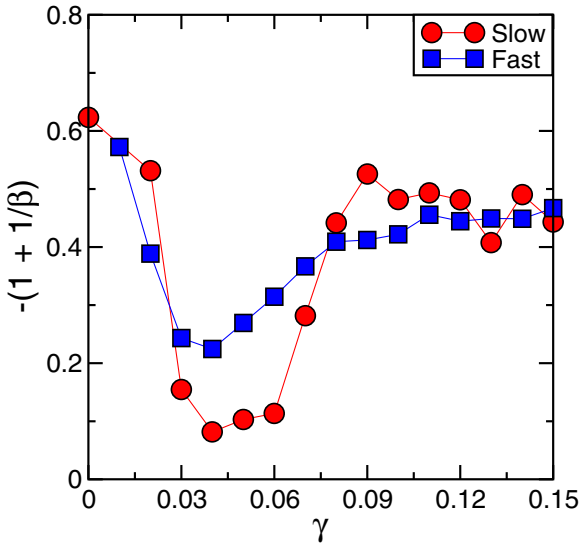

FIG. 2. (Color online) A plot of $-(1+\frac{1}{\beta})$ obtained from the direct measurement of β as a function of γ. Results for the slow quench are shown in circles and for the fast quench in squares. We argue in this paper that these results suffer from severe finite size effects and in reality this figure should be replaced by Fig. 6.

with the scaling law (3). This is equally valid for the slow and the fast quench (see the results of the PDFs for the slow quench in Fig. 4). The results shown in Fig. 2 should be read with this in mind; due to system size and crossover effects the sharp transition at $\gamma = 0^+$ is smeared out, and so is the transition near γ_Y. Clearly, in the case of the fast quench the transitions are even more smeared out. We propose that in the case of slow quench, in the first transition η tries to reach the value 0 and in the second transition the scaling law (3) breaks down and β settles on the value $-2/3$. The theoretical predictions will be presented below in Fig. 6 after the considerations leading to these assertions become clear.

III. THEORETICAL CONSIDERATIONS

A. Relation to the Hessian matrix and its eigenvalues

To understand the statistics of $\Delta\gamma$ we need to connect it to the statistics of the eigenvalues of the Hessian matrix [14,15]. The latter is crucial for the understanding of athermal plasticity. Each plastic instability is due to a saddle-node bifurcation in which an eigenvalue λ_i of the associated Hessian matrix $\mathcal{H}_{ij} = \frac{\partial^2 U}{\partial \mathbf{r}_i \partial \mathbf{r}_j}$ of the potential energy U softens and becomes zero at some value of $\gamma = \gamma_P$. The eigenvalue that becomes zero is not necessarily the lowest eigenvalue of the Hessian when the system is unstrained at $\gamma = 0$. But it always becomes the smallest eigenvalue when the instability is approaching. The modes whose eigenvalues become zero at some value of the external strain are referred to as plastic modes [9–11]. One should be aware that every disordered solid has also Debye modes whose eigenvalues remain roughly independent of the external strains. For the plastic modes, because we are dealing with a saddle-node instability, we know (and see below for details) that $\Delta\gamma_i \sim \lambda_i^2$ and also for the energy barrier ϵ_i the associated saddle-node instability scales as $\epsilon_i \sim \lambda_i^3$. Analyzing

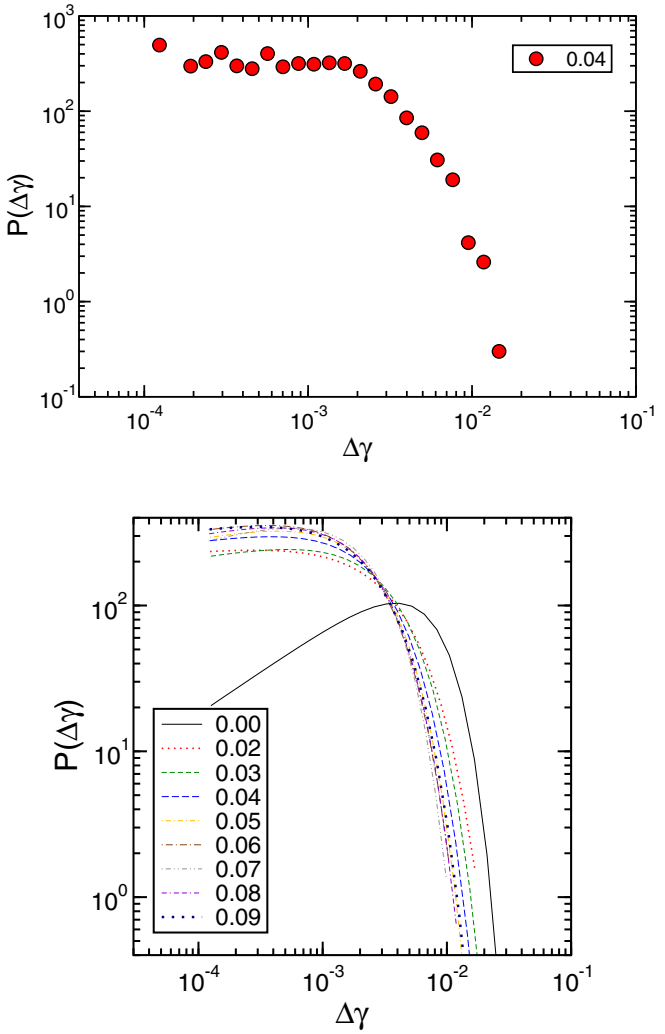

FIG. 3. (Color online) Results for the slow quench. Upper panel: an example of the raw data for the probability distribution functions $P(\Delta\gamma;\gamma)$ for $\gamma = 0.04$. Lower panel: the fits to the PDFs $P(\Delta\gamma;\gamma)$ for a range of values of γ from $\gamma = 0$ to $\gamma = 0.9$ (beyond the plastic yield). Only at $\gamma = 0$ the distribution is Weibull with $\eta \approx 0.6$. For all other values of γ we find $\eta = 0$. This value is explained by the theory in Sec. III.

the properties of an ensemble of the lowest eigenvalues of the plastic modes of the Hessian matrix at fixed strain γ will yield (in the thermodynamic limit) a distribution $P(\lambda;\gamma)$. Knowing the tail of this PDF for $\lambda \to 0$,

$$\lim_{\lambda\to 0} P(\lambda;\gamma) \sim \lambda^{\theta}\ , \tag{5}$$

will allow the calculation of the tails of the distribution of the strain events $P(\Delta\gamma;\gamma)$ at fixed γ and the tail of the associated energy barrier distribution $P_{\epsilon}(\epsilon;\gamma)$ at fixed γ. We reiterate that the distribution $P(\lambda;\gamma)$ discussed here refers to the minimal eigenvalues that are exposed in the tail of the distribution as they tend to zero due to plastic processes. There may be other putative plastic modes that are not yet ready to express their potential instability, and these are not taken into account here. A good example of these plastic modes are those discussed explicitly in Ref. [12].

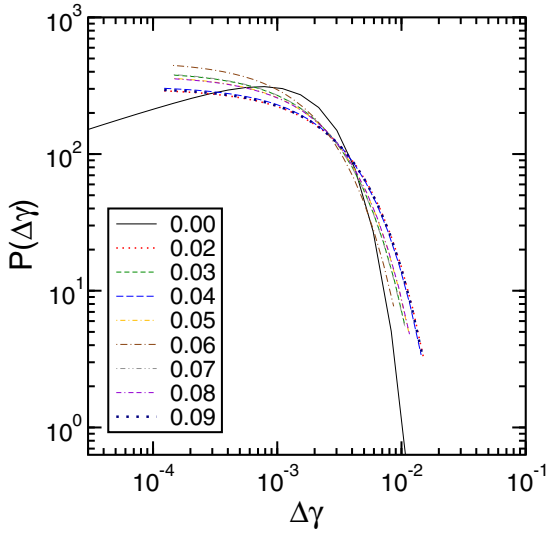

FIG. 4. (Color online) Results for the fast quench: the probability distribution functions $P(\Delta\gamma;\gamma)$ for a range of values of γ from $\gamma = 0$ to $\gamma = 0.9$ (beyond the plastic yield). Only at $\gamma = 0$ the distribution is Weibull with $\eta \approx 0.3$. For all other values of γ we find $\eta = 0$. This value is explained by the theory in Sec. III.

It is very important to keep separate in one's mind two sets of experiments. In the situation described above the strain γ is fixed at some value and an ensemble of $\Delta\gamma_i$ measured. A second experiment involves ramping up γ from zero and measuring consecutive reversible $\Delta\gamma_i$ followed by avalanching. The nth such event will occur at $\gamma = \Sigma_{i=1}^{n}\Delta\gamma_i$. In such an experiment the stochastic dynamics will prove to be very similar to particles drifting in a one-dimensional flow together with added shot noise (with the eigenvalue λ representing the particle "coordinate" and γ equivalent to time). In the thermodynamic limit, when the distribution of eigenvalues of the Hessian becomes a density, we will employ a Fokker-Planck equation for $P(\lambda;\gamma)$, which is similar in structure to a one dimensional flow for λ with an adsorbing boundary at $\lambda = 0$ due to the associated saddle-node instability followed by reinjection of the of a new eigenvalue with a distribution $j_{\rm in}(\lambda,\gamma)$ in order to conserve probability. Its generic form will be

$$\partial P/\partial\gamma = -\partial[v(\lambda,\gamma)P]/\partial\lambda + D(\gamma)\partial^2 P/\partial\lambda^2 + j_{\rm in}(\lambda,\gamma). \tag{6}$$

For understanding the scaling properties of $P(\lambda;\gamma)$ it is crucial to derive the scaling form of $v(\lambda,\gamma)$ which we discuss next. The noise term in this equation models the changes in the distribution function when an eigenvalue hits zero, disappears, and is being replaced by another eigenvalue of the Hessian. When this happens all the eigenvalues change to some extent; this is modeled by the diffusion term above. An important point that will be used below is that this noise term is not expected to show any singular behavior when the eigenvalue of the Hessian is approaching zero.

B. The rate of change of the eigenvalues and the resulting scaling relations

The central result that will be used in the present context is an "equation of motion" for the change in the minimal

eigenvalues of the Hessian matrix upon increasing strain. This equation was derived in Ref. [9], and it turns out to be rather complex. Nevertheless, in the limit of $\lambda \to 0$ this equation can be simplified to exhibit only the most singular contribution, correct up to less singular terms:

$$\frac{d\lambda}{d\gamma} \simeq -\frac{a(\gamma)}{\lambda} + \text{less singular terms}. \tag{7}$$

Together with the boundary condition that λ vanishes at some strain value γ_P, i.e., $\lambda(\gamma_P) = 0$, we integrate Eq. (7) to obtain

$$\lambda(\gamma) = \sqrt{2a(\gamma_P)(\gamma_P - \gamma)} + \text{higher order terms}. \tag{8}$$

We can also expand the projection of the potential energy in the direction that is becoming unstable for $\gamma \to \gamma_P$:

$$U = U_0 + \tfrac{1}{2}\lambda s^2 + \tfrac{1}{6} b s^3 + O(s^4). \tag{9}$$

This form implies that a saddle point exists at $s_\star = -\frac{2\lambda}{b}$, of magnitude

$$\Delta E \equiv U(s_\star) - U_0 \simeq \frac{2\lambda^3}{3b^2} = \frac{4\sqrt{2}}{3}\sqrt{\frac{a^3}{b^4}}\,(\gamma_P - \gamma)^{\frac{3}{2}}, \tag{10}$$

where we have used the solution Eq. (8) for the γ dependence. Equations (8) and (10) are the basic relations from which the scaling relations by which the strain increases, and energy barriers are related to λ,

$$\Delta\gamma \sim \lambda^2, \tag{11}$$

$$\epsilon \sim \lambda^3, \tag{12}$$

can be found. In particular Eq. (11) leads to the obvious scaling relation

$$\eta = (\theta - 1)/2. \tag{13}$$

We expect the scaling relation (13) to be valid for all values of γ and for all amorphous solids since it stems from the saddle-node nature of the plastic events, which is generic.

C. Consequences for the Fokker-Planck equation

The upshot of the preceding discussion is that we can estimate the most singular form of the "speed" $v(\lambda;\gamma)$ in Eq. (6) as

$$v(\lambda;\gamma) \approx -a(\gamma)/\lambda + \text{less singular terms}. \tag{14}$$

We therefore rewrite Eq. (6) in the form

$$\partial P/\partial\gamma \approx a(\gamma)\partial[P/\lambda]/\partial\lambda + D(\gamma)\partial^2 P/\partial\lambda^2 + j_{\rm in}(\lambda,\gamma) \tag{15}$$

with a probability flux

$$J(\lambda,\gamma) = -a(\gamma)P/\lambda - D(\gamma)\partial P/\partial\lambda. \tag{16}$$

The diffusive term in the Fokker-Planck equation results from the "less singular terms" in Eq. (14). Note that we should seek solutions of this equation with an adsorbing boundary condition at $\lambda = 0$, leading to

$$P(\lambda = 0,\gamma) = 0, \tag{17}$$

but with a finite flux for any value of γ. We stress that we have added a nonsingular (in λ) diffusion term to the drift term in the Fokker Planck equation. The reason is that the theory leading to Eq. (14) does not indicate the existence of any other singular term in the "noise" on top of the leading, explicit $1/\lambda$ term in Eq. (14). The most singular contribution is already there. For the same reason also the injection term $j_{\rm in}(\lambda,\gamma)$ is taken as nonsingular.

Accepting the fact that for any value of $\gamma > 0$ the flux must be finite, a direct consequence of the form of Eq. (16) is that $P(\lambda;\gamma)$ *must* start linearly in λ in order to have a finite flux which is neither zero nor infinity:

$$\lim_{\lambda\to 0} P(\lambda;\gamma) \sim \lambda. \tag{18}$$

Using the scaling relation (13) we conclude that $\eta = 0$ for any value of $\gamma > 0$. This result rationalizes entirely the data shown in Fig. 3.

The same conclusion can be obtained directly by analyzing the PDF in the steady-state plastic flow. There both $D(\gamma)$ and $j_{\rm in}(\lambda,\gamma)$ must become γ independent, and we will assume a constant reinjection rate $j_{\rm in}(\lambda) = j_{\rm in}$ between $0 < \lambda < \lambda_{\rm max}$ in line with the avalanching process that occurs in the dynamics, while $j_{\rm in}(\lambda) = 0$ otherwise. We need to solve

$$0 = a_{ss}\partial[P/\lambda]/\partial\lambda + D_{ss}\partial^2 P/\partial\lambda^2 + j_{\rm in}(\lambda). \tag{19}$$

together with Eq. (17). The solution is given by

$$P_{ss}(\lambda) = \frac{6}{\lambda_{\rm max}}[(\lambda/\lambda_{\rm max}) - (\lambda/\lambda_{\rm max})^2] \tag{20}$$

as a quick substitution will confirm. It is properly normalized and $\langle\lambda\rangle = \lambda_{\rm max}/2$. Choosing the same value for $\langle\lambda\rangle$ for both the isotropic and steady-state distributions yields Fig. 5. In addition, for this solution the probability flux J at the adsorbing boundary and the required reinjection rate $j_{\rm in}$ are,

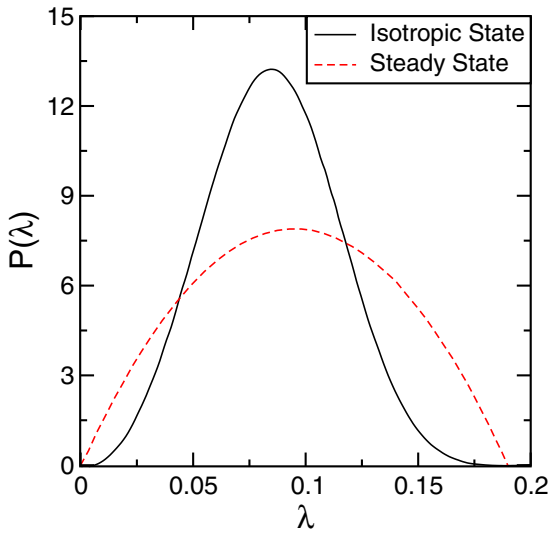

FIG. 5. (Color online) Plots of the isotropic Weibull distribution and the steady-state distribution assuming that the new eigenvalues are equally distributed between $\lambda = 0$ and $\lambda = \lambda_{\rm max}$. The distributions have been chosen so that $\langle\lambda\rangle_{\rm iso} = \langle\lambda\rangle_{ss}$.

respectively,

$$J = \frac{-6(a_{ss} + D_{ss})}{\lambda_{\max}^2},$$
$$j_{\rm in} = \frac{6(a_{ss} + 2D_{ss})}{\lambda_{\max}^3}. \quad (21)$$

The important thing to notice is that the conclusion Eq. (18) is valid also in the steady state, i.e., that $\theta = 1$ and $\eta = 0$.

We thus conclude that there exists a discontinuous transition at $\gamma = 0^+$ such that the Weibull distribution is swept in favor of a distribution that can support a finite flux at $\lambda = 0$. For completeness we discuss the evolution of the PDF upon straining in the Appendix.

IV. CONCLUSIONS

Our analysis of a generic two-dimensional system indicated the existence of three types of solutions:

(i) At $\gamma = 0$ an isotropic Weibull solution

$$P_w(\lambda) = \frac{(1+\theta)}{\langle\lambda\rangle}(\lambda/\langle\lambda\rangle)^{\theta} \exp -(\lambda/\langle\lambda\rangle)^{1+\theta} \quad (22)$$

exists which is singular as $\lambda \to 0$ and for which there is no current; $J = 0$ as $\theta \approx 2.2$ in the case of slow quench. In this state of mechanical equilibrium both the scaling law (3) **and** the scaling law (13) are obeyed.

(ii) For any strain not equal to zero the statistics is fundamentally different. For any value of the strain, both before and after the plastic yield there exists a finite flux of eigenvalues towards $\lambda = 0$ where there is an absorbing boundary condition. This requires $\theta = 1$. Both the scaling laws (3) and (13) appear to hold as long as $\gamma < \gamma_{\rm Y}$. Consequently we expect to find $\eta = 0$ in agreement with the numerical simulations. If the scaling law (3) is still obeyed, we expect to find $\beta = -1$. The direct numerical simulation found $\beta \approx -0.92$ (cf. Fig. 1, middle panel). We ascribe this and the smooth fall down to this value in Fig. 2 to finite size effects.

(iii) Contrary to the analysis shown in the Appendix of the breakdown of the Weibull distribution, we do not have a similar analysis of the yielding transition. It was, however, possible to solve for the steady state PDF in the form of Eq. (20). This solution will be valid for $\gamma > \gamma_Y$. Indeed, here $\theta = 1$ (compared to $\theta = 2.2$ in the isotropic case) and there is a steady-state flux through the system. The actual shape of $P_{ss}(\lambda)$ is not universal for large λ and will depend on the form of the injection feeding $j_{\rm in}(\lambda)$. In Fig. 5 we have assumed constant feeding for all $\lambda < \lambda_{\max} = 2\langle\lambda\rangle$. In contrast the shape for small λ is expected to be universal. Since $\theta = 1$ we expect and find in this range $\eta = 0$ due to the ubiquitous scaling law (13). On the other hand, the scaling law (3) does *not* hold in the flowing steady state. This scaling law stems from the independence of plastic events for $\gamma < \gamma_{\rm Y}$, and it fails in the steady state due to the build-up of correlations between the subextensive plastic events. We thus expect $\beta = -2/3$ universally in this regime, in contradiction with the scaling law (3). Our expectation for the theoretical dependence of β on γ is thus shown in Fig. 6.

Finally, a word of caution is called for. As explained above in several occasions it is the distribution of minimal eigenvalues of the Hessian that is the focus of our analysis. There is another distribution that may be at play here, i.e., the full distribution of plastic modes. This may have a different form and may be associated with other exponents. We assumed that the exponent β is associated with the distribution of minimal eigenvalues. It remains to be seen whether one can determine the full distribution of plastic modes and how that distribution is related to the system-size dependence of $\langle\Delta\gamma\rangle$. At this point the full distribution of the eigenvalues of the plastic modes is not available for a generic amorphous solid. It will be certainly worthwhile to find new methods of determining it.

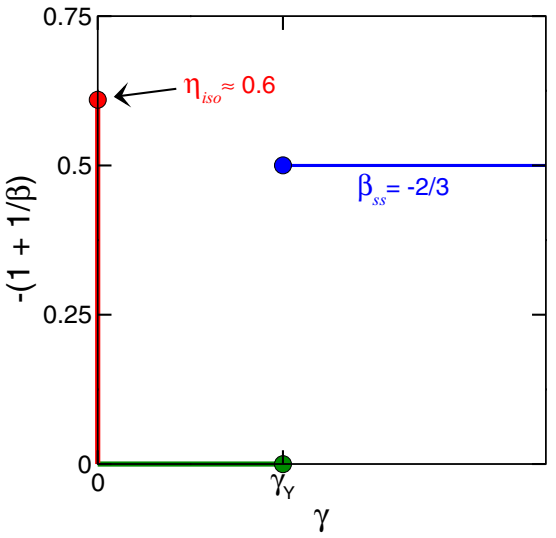

FIG. 6. (Color online) Schematic presentation of the theoretical prediction for the γ dependence of $-(1 + 1/\beta)$. We reiterate that the value of this exponent at $\gamma = 0$ is *not* universal, whereas in the steady state it is universal.

ACKNOWLEDGMENTS

This work has been supported in part by an European Research Council "ideas" grant STANPAS. We thank Edan Lerner and Matthieu Wyart for useful discussions.

APPENDIX: THE EVOLUTION OF THE PROBABILITY DISTRIBUTION BELOW YIELD

In order to study qualitatively the evolution of the probability distribution below we shall examine the simplest Fokker-Planck equation consistent with a singular drift velocity due to the saddle-node dynamics under strain,

$$\partial P/\partial\gamma \approx a\partial[P/\lambda]/\partial\lambda + D(\gamma)\partial^2 P/\partial\lambda^2 + j_{\rm in}(\lambda;\gamma), \quad (A1)$$

and we wish to study the evolution from the initial condition which is the isotropic Weibull distribution valid at $\gamma = 0$ and given by Eq. (22). Thus

$$P(\lambda;\gamma = 0) = P_w(\lambda). \quad (A2)$$

The easiest way to do this is to define the linear Liouville operator

$$L = a\partial[1/\lambda]/\partial\lambda + D\partial^2/\partial\lambda^2 \quad (A3)$$

in terms of which we can rewrite Eq. (A1) as

$$\partial P/\partial\gamma = LP + j_{\rm in}(\lambda;\gamma). \quad (A4)$$

This equation has the general solution $P = P_{\rm hom} + P_{\rm inhom}$ where

$$P_{\rm hom}(\lambda;\gamma) = e^{\gamma L} P_w(\lambda),$$
$$P_{\rm inhom}(\lambda;\gamma) = e^{\gamma L}\int_0^{\gamma} e^{-\gamma' L} j_{\rm in}(\lambda;\gamma')\, d\gamma'. \quad \text{(A5)}$$

The inhomogenous solution depends on the structure of the injection rate $j_{\rm in}(\lambda,\gamma)$ and is not universal. The only thing we really know is that the reinjection rate must ensure conservation of probability. We shall take the constant reinjection rate $j_{\rm in}(\lambda,\gamma) = j_{\rm in}(\gamma)$ between $0 < \lambda < \lambda_{\rm max}$ in line with the avalanching process that occurs in the dynamics, while $j_{\rm in}(\lambda,\gamma) = 0$ otherwise, and consequently

$$P_{\rm inhom}(\gamma) = \int_0^{\gamma} j_{\rm in}(\gamma')\, d\gamma', \quad \text{(A6)}$$

where $j_{\rm in}(\gamma')$ is fixed by the requirement that probability is conserved. As $P(\lambda,\gamma) = P_{\rm hom}(\lambda;\gamma) + P_{\rm inhom}(\gamma)$, we see that on integrating this expression between $0 < \lambda < \lambda_{\rm max}$ that

$$1 = \int_{\sqrt{2a\gamma}}^{\lambda_{\rm max}} P_{\rm hom}(\lambda;\gamma)\, d\lambda + \lambda_{\rm max} P_{\rm inhom}(\gamma)\, d\lambda, \quad \text{(A7)}$$

and this yields an expression for $j_{\rm in}(\gamma)$,

$$j_{\rm in}(\gamma) = \frac{-1}{\lambda_{\rm max}} d\left[\int_{\sqrt{2a\gamma}}^{\lambda_{\rm max}} P_{\rm hom}(\lambda;\gamma) d\lambda\right] \Big/ d\gamma. \quad \text{(A8)}$$

Note that the lower bound of the integral involving $P_{\rm hom}$ extends only to $\sqrt{2a\gamma}$. This (as we will see below) is because $P_{\rm hom}(\lambda < \sqrt{2a\gamma};\gamma) = 0$.

The homogenous solution shows the evolution of the Weibull distribution under straining it and obeys

$$P_{\rm hom}(\lambda;\gamma) = e^{\gamma L} P_w(\lambda) = \int_0^{\infty} dx\, P_w(x) e^{\gamma L}\delta(x-\lambda), \quad \text{(A9)}$$

The Liouville operator acting on the delta function $e^{\gamma L}\delta(x-\lambda) = \frac{1}{\sqrt{4\pi D\gamma}} \exp(-\frac{[x-\tilde{\lambda}(\lambda;\gamma)]^2}{4D\gamma})$ will transform it into a Gaussian. In Eq. (A9) the expression $\tilde{\lambda}(\lambda;\gamma) = \sqrt{\lambda^2 - 2a\gamma}$ is the value that an eigenvalue λ assumes due to drift alone. Thus we can rewrite Eq. (A9) as

$$P_{\rm hom}(\lambda;\gamma) = \frac{1}{\sqrt{4\pi D\gamma}} \int_0^{\infty} dx\, P_w(x) \exp\left(-\frac{[x-\tilde{\lambda}(\lambda;\gamma)]^2}{4D\gamma}\right). \quad \text{(A10)}$$

Using the new variable t where $x = \tilde{\lambda}(\lambda;\gamma) + \sqrt{4D\gamma}t$ we can rewrite Eq. (A10) as

$$P_{\rm hom}(\lambda;\gamma) = \frac{1}{\sqrt{\pi}} \int_{\frac{-\tilde{\lambda}(\lambda;\gamma)}{\sqrt{4D\gamma}}}^{\infty} dt\, P_w[\tilde{\lambda}(\lambda;\gamma) + \sqrt{4D\gamma}t] \exp(-t^2). \quad \text{(A11)}$$

From Eq. (A11) we see that as $\lambda \to \sqrt{2a\gamma}$ from above we find

$$P_{\rm hom}(\sqrt{2a\gamma};\gamma) = \frac{1}{\sqrt{\pi}} \int_0^{\infty} dt\, P_w(\tilde{\lambda}\sqrt{4D\gamma}t) \exp(-t^2), \quad \text{(A12)}$$

because here $\tilde{\lambda} = 0$. But for $\lambda < \sqrt{2a\gamma}$ there is no solution. Any nonzero value for $P(\lambda < \sqrt{2a\gamma},\gamma)$ must come from feeding combined with flow from $\lambda = \sqrt{2a\gamma}$ and adsorption at $\lambda = 0$ resulting in the boundary condition $P(\lambda = 0,\gamma) = 0$.

On the other hand if $\lambda \gg \sqrt{2a\gamma}$, the Weibull term $P_w[\tilde{\lambda}(\lambda,\gamma) + \sqrt{4D\gamma}t]$ can be expanded in powers of t inside the integral representation for $P_{\rm hom}$ given by Eq. (A11) as the exponential $\exp -t^2$ will ensure that only values of $t \ll 1$ are important. In this manner an expansion in terms of the gradients of the Weibull distribution can be derived. To second order we find

$$P_{\rm out}(\lambda;\gamma) = C_1(\lambda;\gamma) P_w(\tilde{\lambda}(\lambda;\gamma)) + C_2(\lambda,\gamma) P_w(\tilde{\lambda}(\lambda;\gamma))' + C_3(\lambda;\gamma) P_w(\tilde{\lambda}(\lambda;\gamma))'', \quad \text{(A13)}$$

where

$$C_1(\lambda;\gamma) = [1 + \mathrm{erf}[\tilde{\lambda}(\lambda;\gamma)/\sqrt{4D\gamma}]]/2,$$
$$C_2(\lambda;\gamma) = \sqrt{D\gamma/\pi}\, \exp[-\tilde{\lambda}(\lambda;\gamma)^2/(4D\gamma)],$$
$$C_3(\lambda;\gamma) = (D\gamma/2)\{1 - \tilde{\lambda}(\lambda;\gamma)/\sqrt{(\pi D\gamma)} \times \exp[-\tilde{\lambda}(\lambda;\gamma)^2/4D\gamma] + \mathrm{erf}[\tilde{\lambda}(\lambda;\gamma)/\sqrt{4D\gamma}]\}, \quad \text{(A14)}$$

and the error function is given by $\mathrm{erf}(x) = (2/\sqrt{\pi})\int_0^x \exp(-t^2)\, dt$. Note once again that an examination of Eq. (A13) shows that this solution becomes singular when $\tilde{\lambda}(\lambda;\gamma) = 0$ or for $\lambda < \sqrt{2a\gamma}$. In other words this solution is also valid only for $\lambda > \sqrt{2a\gamma}$. Thus for any $\gamma \neq 0$ a growing region exists where the Weibull solution breaks down. It is for this reason that we have written $P_{\rm hom} = P_{\rm out}$ in Eq. (A13) to represent the outer solution of the distribution.

We note there appears to exist a growing boundary layer with an inner solution $P_{\rm in}(\lambda,\gamma)$ for $\lambda < \sqrt{2a\gamma}$. To solve for this inner solution we write

$$P_{\rm in}(\lambda;\gamma) = \Sigma_n A_n(\gamma)\lambda^n \quad \text{(A15)}$$

and substitute in Eq. (A1). For $\lambda < \sqrt{2a\gamma}$, the Weibull distribution is swept away to to be replaced by essentially a constant flux distribution $P_{\rm in}(\lambda;\gamma) \approx A_1(\gamma)\lambda$ for small λ. In that case, by matching solutions at $\lambda = \sqrt{2a\gamma}$ we would find $A_1(\gamma) \approx P_{\rm out}(\sqrt{2a\gamma},\gamma)/\sqrt{2a\gamma}$ due to fitting of inner and outer solutions. Together these arguments yield

$$P_{\rm in}(\lambda;\gamma) \approx [P_{\rm out}(\sqrt{2a\gamma},\gamma)/\sqrt{2a\gamma}]\lambda. \quad \text{(A16)}$$

As we can approximate Eq. (A12) by its saddle point approximation for small γ we also find

$$P_{\rm hom}(\sqrt{2a\gamma};\gamma) \approx \left[\frac{(2\theta D\gamma)}{e\langle\lambda\rangle^2}\right]^{\theta/2} \sqrt{\frac{4\pi D\gamma}{\langle\lambda\rangle(1+\langle\lambda\rangle)}}. \quad \text{(A17)}$$

We are now in a position to calculate the flux $J(\gamma)$ and find that at small strain it grows in a singular manner as

$$J(\gamma) \sim \gamma^{\theta/2}. \quad \text{(A18)}$$

[1] F. Varnik, L. Bocquet, and J.-L. Barrat, J. Chem. Phys. **120**, 2788 (2004); D. Rodney and C. A. Schuh, Phys. Rev. B **80**, 184203 (2009); C. E. Maloney and A. Lemaître, Phys. Rev. E **74**, 016118 (2006).

[2] D. L. Malandro and D. J. Lacks, J. Chem. Phys. **110**, 4593 (1999); C. Maloney and A. Lemaitre, Phys. Rev. Lett. **93**, 016001 (2004); H. G. E. Hentschel, S. Karmakar, E. Lerner, and I. Procaccia, *ibid.* **104**, 025501 (2010).

[3] S. Karmakar, E. Lerner, and I. Procaccia, Phys. Rev E **82**, 055103(R) (2010).

[4] E. Lerner and I. Procaccia, Phys. Rev. E **79**, 066109 (2009).

[5] J. Lin and M. Wyart, arXiv:1506.03639v2.

[6] J. Lin, T. Gueudré, A. Rosso, and M. Wyart, Phys. Rev. Lett. **115**, 168001 (2015).

[7] For an example see K. Ramola, K. Damle, and D. Dhar, Phys. Rev. Lett. **114**, 190601 (2015).

[8] See, for example, T. Kawasaki and L. Berthier, arXiv:1507.04120.

[9] H. G. E. Hentschel, S. Karmakar, E. Lerner, and I. Procaccia, Phys. Rev. E **83**, 061101 (2011).

[10] S. Karmakar, E. Lerner, and I. Procaccia, Physica A **391**, 1001 (2012).

[11] R. Gutiérrez, S. Karmakar, Y. G. Pollack, and I. Procaccia, Europhys. Lett. **111**, 56009 (2015).

[12] L. Gartner and E. Lerner, arXiv:1507.06931v1.

[13] O. Gendelman, P. K. Jaiswal, I. Procaccia, B. Sen Gupta, J. Zylberg, Europhys. Lett. **109**, 16002 (2015).

[14] V. Gurarie and J. T. Chalker, Phys. Rev. B **68**, 134207 (2003).

[15] M. Baity-Jesi, V. Martín-Mayor, G. Parisi, and S. Pérez-Gaviro, arXiv:1506.04927v1.